

# Immune Subtypes and Characteristics of Endometrial Cancer Based on Immunogenes

Chong Zhang, Jianqing Xu, Ming Wang, Yue He, Yumei Wu

Department of Gynecologic Oncology, Beijing Obstetrics and Gynecology Hospital, Capital Medical University, Beijing Maternal and Child Health Care Hospital, Beijing, People's Republic of China

Correspondence: Yumei Wu, Department of Gynecologic Oncology, Beijing Obstetrics and Gynecology Hospital, Capital Medical University, Beijing Maternal and Child Health Care Hospital, 17 Qihelou St, Dongcheng District, Beijing, 100006, People's Republic of China, Email [wym597118@ccmu.edu.cn](mailto:wym597118@ccmu.edu.cn)

**Purpose:** The aim of this study was to explore the immune subtypes of endometrial cancer (EC) and its characteristics by immunogenes from the perspective of multidimensional genomics (multi-omics).

**Patients and Methods:** Immune subtypes were carried out using an unsupervised non-negative matrix factorization clustering (NMF) method and their characteristics were analysed. Key genes were identified using random forest analysis. A predictive model for immune subtypes and their clinical prognosis were constructed. The relationship between immune subtypes and molecular subtypes was investigated.

**Results:** Two immune subtypes C1 and C2 were available. C2 patients were younger, less graded, had significantly higher immune cell infiltration, immune checkpoint expression, tumor neoantigens, tumor mutation load than C1 ( $P < 0.05$ ). S100A9, CD3D, CD3E, HLA-DRB1 and IL2RB were the key genes with significant survival outcomes. S100A9 expression was lower in C2 than C1, and IL2RB, HLA-DRB1, CD3E and CD3D expression was higher than C1 ( $P < 0.05$ ). The predictive accuracy of five key genes for immune subtypes was good, with a Receiver operating characteristic of 0.941. The incidence of TP53abn type in C2 was significantly lower than that of C1, and the incidence of POLE type was significantly higher than that of C1 ( $P < 0.0001$ ).

**Conclusion:** EC can be divided into two immune subtypes based on immunogenes. Low expression of S100A9 and high expression of IL2RB, HLA-DRB1, CD3E, and CD3D suggest sensitivity to immunotherapy and a good prognosis.

**Keywords:** endometrial cancer, immune subtype, immunotherapy, multidimensional genomic, tumor immune microenvironment

## Introduction

EC (endometrial cancer) is the sixth most commonly diagnosed cancer in women, with 417,000 new cases and 97,000 deaths in 2020.<sup>1-3</sup> The early diagnosis and prognosis of EC are favorable, with a five-year overall survival rate of 71–80%.<sup>4</sup> However, the prognosis is poor for some patients who are already in the advanced stage when diagnosed.<sup>5</sup> The classification method of EC is gradually moving from traditional clinical and pathological classification to molecular classification. The Cancer Genome Atlas (TCGA) database (<https://portal.gdc.cancer.gov/>) is the largest currently available database of cancer gene information. It stores data including gene expression, miRNA expression, copy number variations, DNA methylation, SNPs, and more. In 2013, TCGA pioneered the molecular typing of EC, with 373 cases of POLE-ultramutated, highly microsatellite unstable status (MSI-H) or mismatch repair deficient (MMRd), copy number low (CNL) or no specific molecular profile (NSMP), and copy number high (CNH) or TP53 subtypes, accounting for 7%, 28%, 39%, and 26%, respectively.<sup>6</sup> POLE-ultramutated and MMRd subtypes with high tumor mutational burden (TMB), there is a correlation with high immunogenicity, which is evidenced by the presence of more tumor-associated specific neoantigens. This leads to an increase in CD3<sup>+</sup> and CD8<sup>+</sup> tumor-infiltrating lymphocytes. The combination of a high mutation load, high tumor-infiltrating lymphocytes, and overexpression of programmed cell death protein 1 (PD-1) makes the EC an ideal target for immunotherapy intervention. This has led to the development of new treatment options, including single-immunotherapy and immunotherapy combined with other treatments, which have the potential to revolutionize cancer treatment. Immunotherapy has become more prominent in recent years.<sup>7</sup> The Food and Drug Administration has approved multiple immune checkpoint inhibitors (ICIs) for routine use in treating advanced or recurrent cancer patients who have failed other treatments in clinical practice since 2014.<sup>8</sup> Currently the National

Comprehensive Cancer Network (NCCN) guidelines in the US recommended patients with MSI-H/MMRd consider pembrolizumab or dostarlimab as a first-line treatment option, while avelumab or nivolumab may be appropriate for those who have progressed on this therapy.<sup>9</sup> The NSMP type has the highest number of cases among the four subtypes, and its treatment is currently uncertain. Consequently, molecular typing cannot, to some extent, screen the most suitable population for immunotherapy. The concept of immune subtypes of EC has been proposed recently. Studies have typed the disease according to immune genes or immune cell infiltration, but they have many limitations.<sup>10–15</sup> This study aims to identify the immune subtypes of EC based on immune genes and analyze their features from a multi-omics perspective.

## Materials and Methods

### Studied Population

The patients of Uterine Corpus Endometrial Carcinoma (UCEC) with the raw mRNA expression data and clinical data including overall survival (OS) were recruited in our study. No restrictions were placed on cancer molecular subtype or surgical stage or TNM stage or histological stage. The raw mRNA expression data processed and clinical data were downloaded from the TCGA database. The progression-free interval (PFI) and disease-free interval (DFI) information of the TCGA-UCEC cohort was obtained from the Xena database (<http://xena.ucsc.edu/>). The IMvigor210 dataset was obtained from the IMvigor210CoreBiologies package (<http://researchpub.gene.com/IMvigor210CoreBiologies/IMvigor210CoreBiologies>), which provided 348 case samples with complete prognostic information and a survival time greater than 0.<sup>16</sup> The TCGA-UCEC cohort, consisting of 554 patients, was used as the training cohort, while three other public cohorts, UCEC-PFI, UCEC-DFI and IMvigor210 dataset, were used as validation cohorts. The immune-related genes used were extracted from the GeneCard Database (<https://www.genecards.org>) based on a Relevance score >1.

### Establishment and Validation of Immune Subtypes

Immunity-related genes were used as the total candidate gene set. The study evaluated the correlation between all candidate genes and OS by Cox regression analysis using the R package “survival” with the clinical information of UCEC patients. Prognostic genes were screened out in EC. NMF clustering method was performed on the TCGA-UCEC dataset based on the expression profiles of prognostic genes.<sup>17</sup>

### Characterization of Immune Subtypes

*Immune signatures:* The study analyzed the immune process using the single sample gene set enrichment analysis (ssGSEA) algorithm, followed by a difference-in-difference analysis to identify the immune signature of a specific subtype.<sup>18</sup>

*Immune scores:* Additionally, the ESTIMATE algorithm was used to calculate immune and stromal scores which reflect the abundance of stromal and immune cell gene signatures.<sup>19</sup>

*Immuno-cell populations:* The study conducted a more detailed analysis of immune infiltration using the Microenvironment cell population-counter and the ssGSEA algorithm. The results were then compared to those from previous immune algorithms. The MCP algorithm evaluated eight immune and two non-immune stromal cell populations, while the GSVA-R software package was used to estimate six additional immune cell populations.<sup>20</sup>

*Pathways:* We analyzed Gene Ontology (GO) and Kyoto Encyclopedia of Genes and Genomes (KEGG) processes using the ssGSEA algorithm.<sup>21</sup> The top 10 pathways with the highest normalised enrichment score (NES) values were selected for presentation. The gene sets were obtained from the MSigDB database (<http://www.gsea-msigdb.org/gsea/downloads.jsp>).

*Drug sensitivity:* Using the “pRRophetic” package, we predicted the chemotherapy sensitivity of each tumor sample based on data from the largest pharmacogenomics database (GDSC, Cancer Drug Sensitivity Genomics Database, <https://www.cancerrxgene.org/>).<sup>22</sup> The regression and prediction accuracy were tested using the GDSC training set with 10-fold cross-validation. Default values were used for all parameters, including the use of “combat” to remove batch effects and taking the mean of duplicate gene expression.

*Mutation, TMB and Immunotherapy:* Exon mutation data for EC were downloaded from TCGA using the maftools package. The mutation maps were obtained using the oncoPrint function of the ComplexHeatmap package. To predict the efficacy of immunotherapy, we measure the similarity of gene expression profiles between our subclasses and previously published samples treated with immunotherapy based on SubMap analysis (gene patterns). The Tumor Immune Dysfunction and Exclusion algorithm was used to predict the impact of immune subtypes on immunotherapy exclusion.<sup>23</sup>

## Key Genes Selection, Model Fitting, Total RNA Extraction, Quantitative Real-Time PCR (qRT-PCR) Analysis and Correlation with TCGA Molecular Subtypes

*Key genes selection:* A Random Survival Forest (RSF) model was created using the randomForestSRC package for feature selection. We also used the RSF algorithm to rank the importance of prognosis-related genes (nrep = 1000, indicating a number of iterations of 1000 in the Monte Carlo simulation). Random forests reliably quantify the relative importance of each variable, and we identified genes with relative importance >0.3 as final key genes.

*Predictive models for immune subtypes and clinical prognosis:* Using the “rms” package and the logistic regression method, a predictive model for immune subtypes of key genes is constructed and a nomogram is drawn. And a calibration curve is drawn and tested (calibration, *U*-test). In addition, we performed univariate Cox regression analysis on the prognosis of immune subtypes based on key genes, and further constructed a prognostic model using lasso regression. Use lasso regression analysis and stratified analysis to test the role of the risk score in predicting patient prognosis. Use bootstrap resampling method for internal validation based on training set and draw calibration plot.

*QRT-PCR analysis:* A total of five tumors and adjacent normal tissues were collected from five patients with EC. The patients were fully informed and provided informed consent. Total RNA was extracted using Total RNA Extraction Kit (Solarbio.R1200), and reverse transcription was performed for qRT-PCR analysis, as previously described.<sup>24</sup> The levels of real-time PCR analysis were quantified using SYBR-Green (Takara, Otsu, Shiga, Japan) and normalised to those of GAPDH. The upstream and downstream primer sequences were as follows:

IL2RB:5'-AGGGCCCTGGAGAGATGG-3' and 5'-CGCCATTACATCCACAGGGT-3'  
HLA-DRB1:5'-TGCAGCACCATAACCTCCTG-3' and 5'-TTGTGGATCAGGCCTGTGG-3'  
S100A9:5'-AGTGGCCAAGATCACAGTGG-3' and 5'-GCCTGGCCTCCTGATTAGTG-3'  
CD3E:5'-GACCTCTGGAGAACTGTC-3' and 5'-ATTCTCTCTCGTGGGGTCCA-3'  
CD3D:5'-GTGGCTGGCATCATTGTCAC-3' and 5'-GCCTTCCAGTCTCATGTCCA-3'

*Relationship between immune subtypes and molecular subtypes:* Statistical analysis was performed on EC patients in the TCGA-EC cohort, including those with microsatellite stable status, gene mutations, copy number variations, clinical features and clinical outcomes. POLE mutation patients were identified as POLE-ultramutated type, highly microsatellite unstable status (MSI-H) patients were identified as MSI-H or MMRd type, TP53 mutation patients were identified as TP53abn, and the remaining patients were classified as molecularly typed as NSMP type. Using the subtypes obtained, the relationship between immune subtypes and molecular subtypes was further analyzed.

## Statistical Analysis

The baseline characteristics and laboratory results of the clinical validation cohort were summarized using descriptive statistical methods, including percentages, mean  $\pm$  standard deviation (SD), and 95% confidence interval (CI). The comparison of differences between two groups of quantitative data is conducted using the *t*-test. Survival curves were generated using the Kaplan-Meier method and compared using the Log rank test. A bioinformatics analysis was conducted using the R language (version 4.0). The in vitro experiments were repeated at least three times. Use SDS software version 2.1 (Applied Biosystem; Thermo Fisher Scientific) to calculate the quantitative circulating fluorescence value Ct, and use the  $2^{-\Delta\Delta Ct}$  method to calculate the relative expression level of the target gene. All statistical tests

were bilateral, with  $p < 0.05$  indicating statistical significance. The comparison of differences between two groups of technical data was conducted using a chi-square test or a rank sum test. All data were analyzed using SPSS 17.0 (SPSS, Inc., Chicago, IL).

## Results

### Studied Population

The normal group ( $n=35$ ), and the tumor group ( $n=554$ ) were included. The 931 immune-related genes used were extracted from the GeneCard Database based on a Relevance score  $>1$ .

### Establishment and Validation of Immune Subtypes

A flow chart was created to describe our study systematically (Figure 1A). Prognostic genes in EC were screened using Cox one-way regression analysis. A total of 106 prognosis-related genes were screened ( $p < 0.05$ ). We clustered the TCGA dataset based on the expression of the above 106 candidate genes using NMF consensus clustering and finally selected  $k = 2$  as the optimal number of clusters after comprehensive consideration (Figure 1B). Subsequent independent validation of the clustering from three extensive validation sets using the  $k = 2$  classification also revealed two distinct molecular typologies. We observed significant prognostic differences in the TCGA dataset, with C2 having a better survival probability compared to C1 ( $p < 0.05$ , Figure 1C). In addition, similar differences were likewise observed in the analysis of the three validation sets, with C2 having a significantly higher survival time than the C1 subgroup ( $p < 0.05$ , Figure 1D-F).

### Characterization of Immune Subtypes

*Immune signatures:* The results showed a clear classification of immune features between the two subgroups, with the C2 subgroup having significantly higher immune features such as B cells, T cells, T helper cells, and Effector Memory T Cell (Tem) than the C1 subgroup ( $p < 0.05$ , Figure 2A and B). In addition, C2 had a higher score related to Angiogenesis pathway activation than C1 ( $p < 0.05$ , Figure 2C).

*Immune scores:* The ESTIMATE algorithm was then used to calculate immune and stromal scores. The immune and stromal scores differed between the two groups and C2 had significantly higher immune and stromal scores than C1 ( $p < 0.05$ , Figure 2D and E).

*Immuno-cell populations:* The abundance of 16 immune-related cell types was calculated and presented in a heat map (Figure 2F). The results showed that there was a significant difference in the level of immune infiltration between the two subtypes, suggesting that the classified immune profiles were reproducible. In addition, T cells, CD8 T cells, Cytotoxic lymphocytes, B lineage, and natural killer cells were significantly higher in the C2 subgroup than in the C1 subgroup ( $p < 0.05$ , Figure 2G). Further investigation of the association between immune types and the expression of 12 potentially targetable immune checkpoint genes, showed that C2 had a higher expression in the fibrinogen-like protein 1, lymphocyte activation gene 3, CD274, programmed cell death protein 1 (PDCD1, PD-1), CD247, programmed cell death protein 1 Ligand 2 immune checkpoints ( $p < 0.05$ , Figure 2H).

*Pathways:* The pathways with higher scores in GO analysis of C2 were mainly IMMUNOGLOBULIN COMPLEX, COMPLEMENT ACTIVATION, ANTIGEN BINDING and other signalling pathways. In contrast, the pathways with higher scores in the KEGG analysis of C2 were mainly signalling pathways such as AUTOIMMUNE THYROID DISEASE, RIBOSOME, and ALLOGRAFT REJECTION.

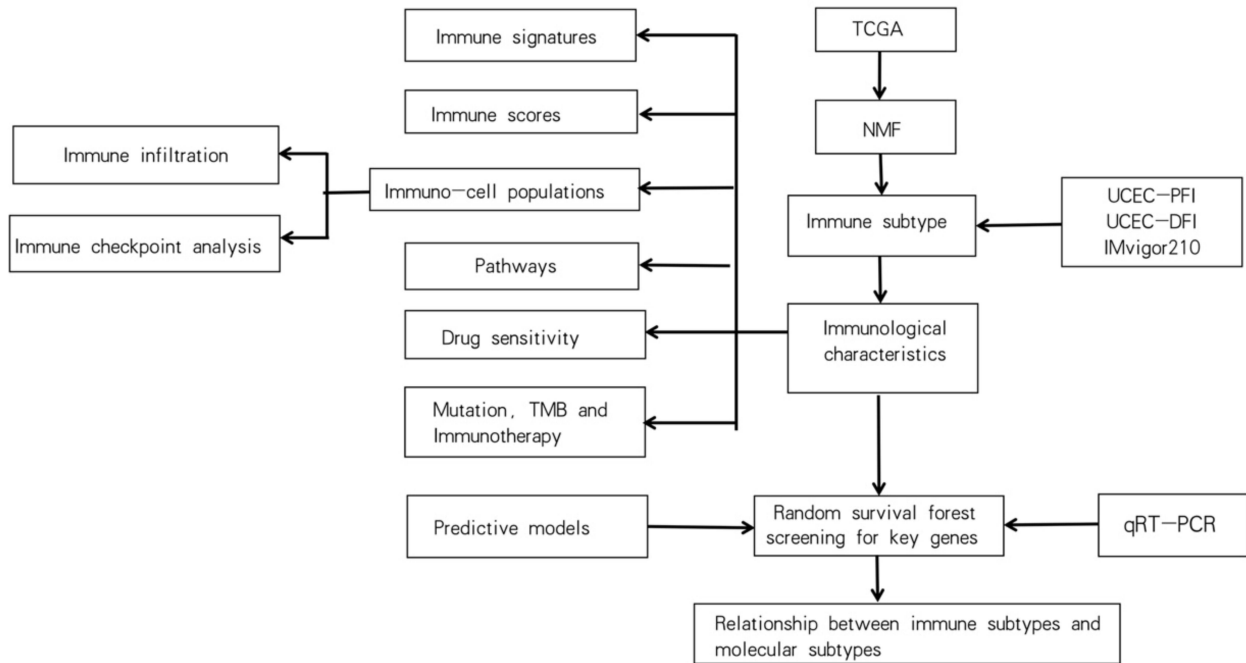
*Drug sensitivity:* Immune subtype was significantly correlated with patient sensitivity to drugs such as BMS.536924, PF.02341066, Roscovitine, Temozolomide, and JNK. Inhibitor.VIII ( $p < 0.05$ ).

*Mutation, TMB and Immunotherapy:* The percentage of mutations in several genes such as Phosphatase and Tensin Homolog deleted on Chromosome 10 (PTEN), Phosphatidylinositol-3-kinase (PIK3CA), AT-Rich Interaction Domain 1A (ARID1A), titin (TTN), Lysine-specific histone methyltransferase 2D etc. was significantly higher in C2 than in C1 ( $p < 0.05$ , Figure 3A). Additionally, TMB was significantly higher in C2 than in C1 ( $p < 0.05$ , Figure 3B and C). C2 was

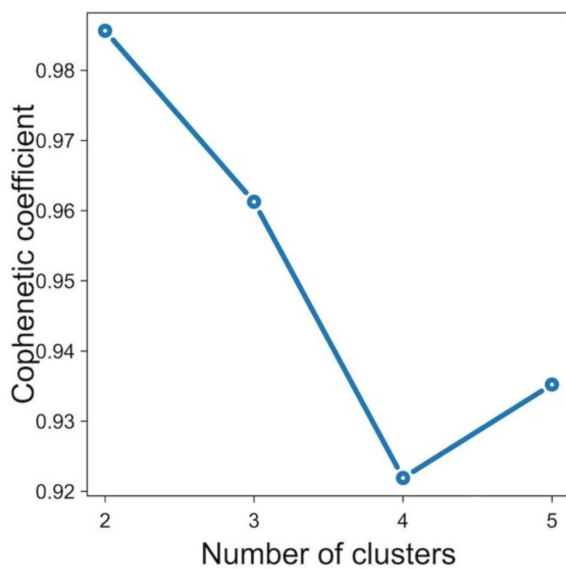


more sensitive to immunotherapy ( $p < 0.05$ , Figure 3D). Analysis of tumor immune rejection revealed differences in the immune subtype, where Exclusion was significantly different between subtypes, with C1 being significantly higher than C2 ( $p < 0.05$ , Figure 3E).

(A)



(B)



(C)

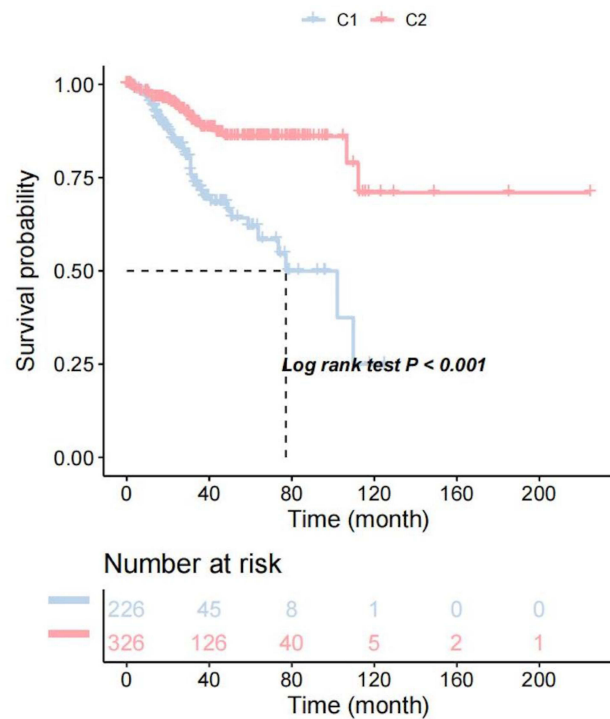
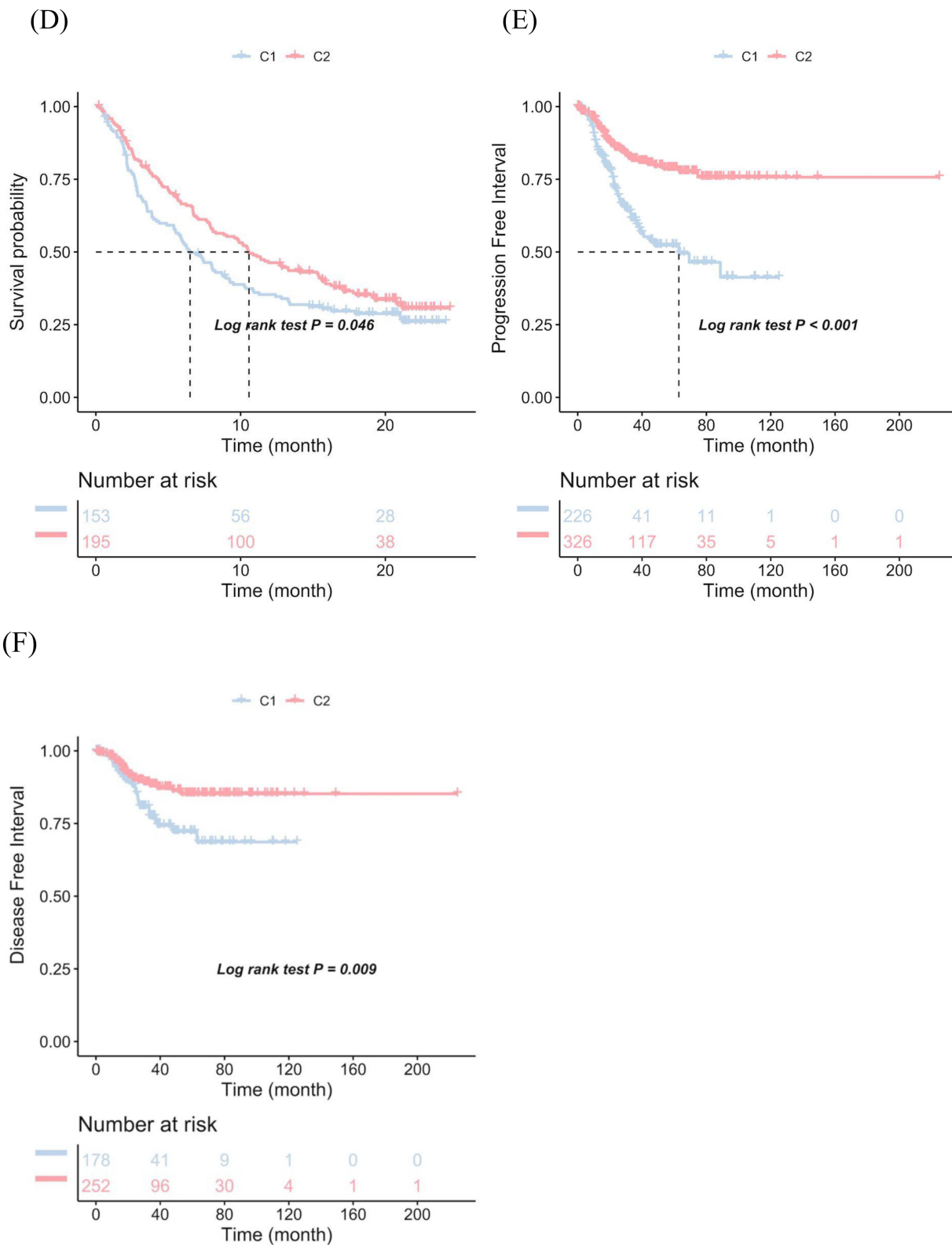


Figure 1 Continue.

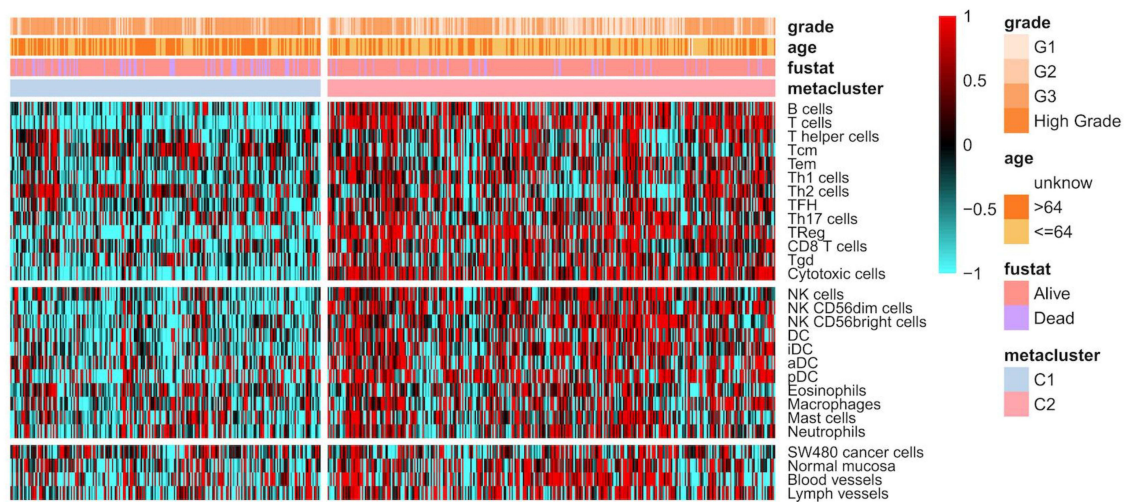


**Figure 1** Establishment and validation of immune subtypes. **(A)** Flow chart of the study. **(B)** Cophenetic coefficient for NMF in TCGA. **(C)** KM curve of metacluster in TCGA. **(D)** KM curve of metacluster in IMOV cohort. **(E)** KM curve of metacluster in PFI cohort. **(F)** KM curve of metacluster in DFI cohort. The statistical significance of differences was determined by Log rank test.

# Key Genes Selection, Model Fitting, Total RNA Extraction, Quantitative Real-Time PCR (qRT-PCR) Analysis and Correlation with TCGA Molecular Subtypes

**Key genes selection:** Differential analysis between the C2 and C1 groups identified 211 downregulated genes and 22 upregulated genes, give a total of 233 differential genes  $p < 0.05$ , Fifteen of these genes were prognostic genes. To further identify the key genes affecting EC, we performed RSF analysis of these 15 overlapping differential genes and we identified the genes with relative importance  $> 0.3$  as the final markers: S100A9, CD3D, CD3E, Human leukocyte antigen (HLA)-DRB1(HLA-DRB1) and interleukin-2 receptor subunit beta (IL2RB) in order of importance (Figure 4A). The KM results of 5 genes were significant ( $p < 0.05$ , Figure 4B-F). S100A9 expression was lower in the C2 group than in the C1 group, and IL2RB, HLA-DRB1, CD3E and CD3D were higher than in the C1 group ( $p < 0.05$ , Figure 4G).

(A)



(B)

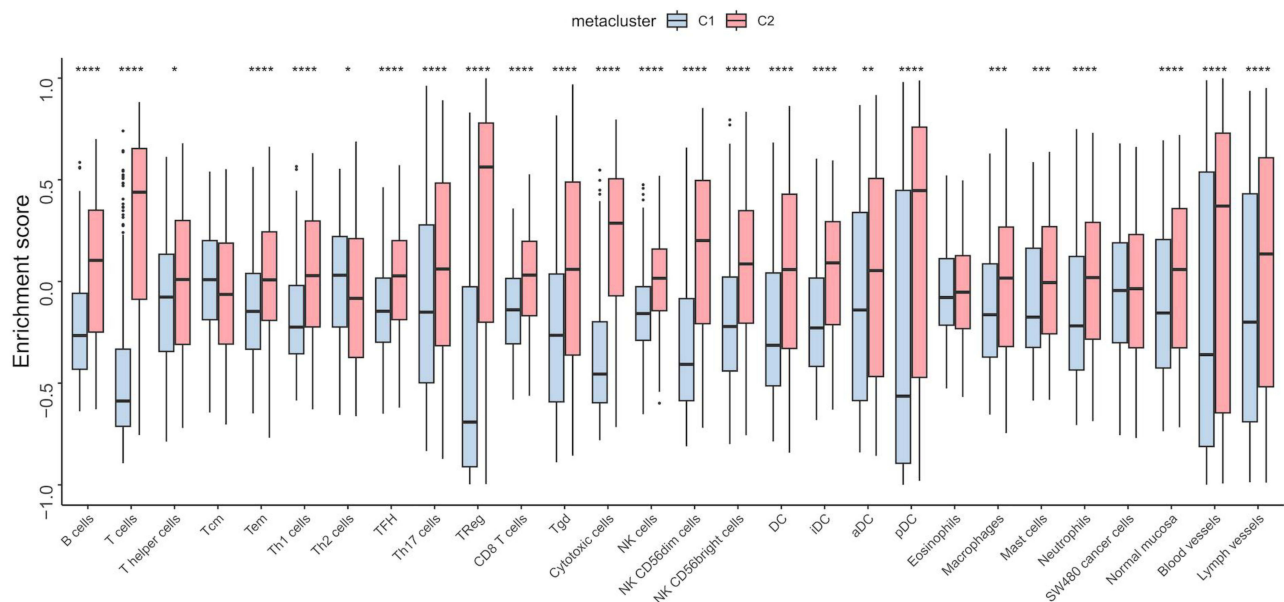
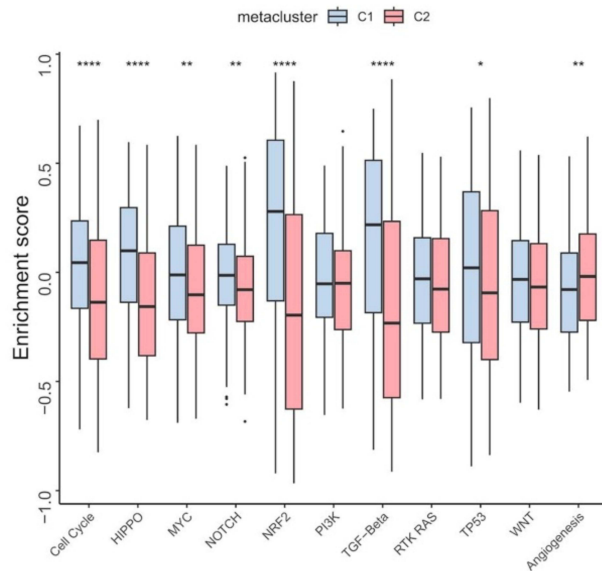


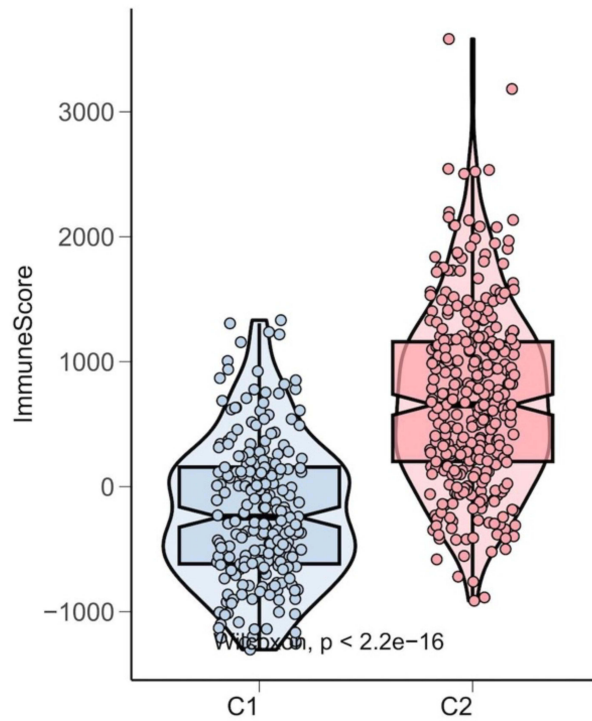
Figure 2 Continue.

*Predictive models for immune subtypes and clinical prognosis:* A predictive model of five key genes for immune subtypes was constructed and a nomogram was drawn (Figure 4H). A calibration curve for verification (calibration, U-test) was drawn (Figure 4I). Its corresponding P-value is S: p. When S:  $p > 0.05$ , it indicates passing the calibration test.

(C)



(D)



(E)

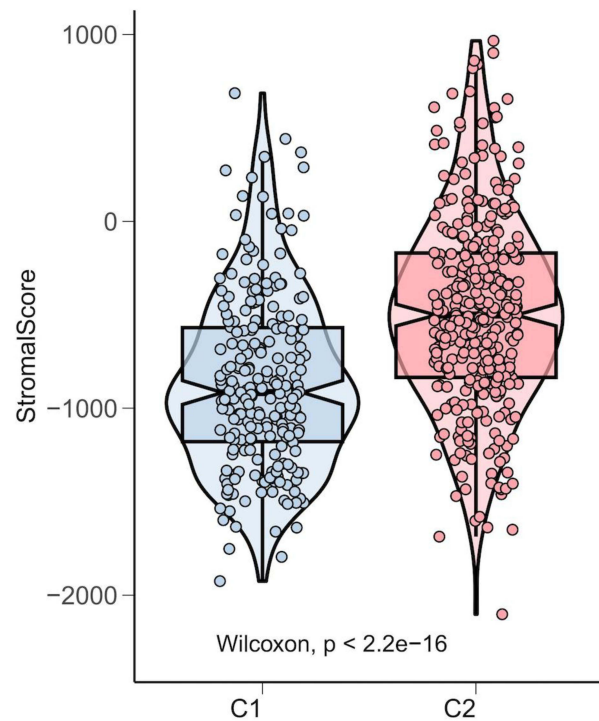
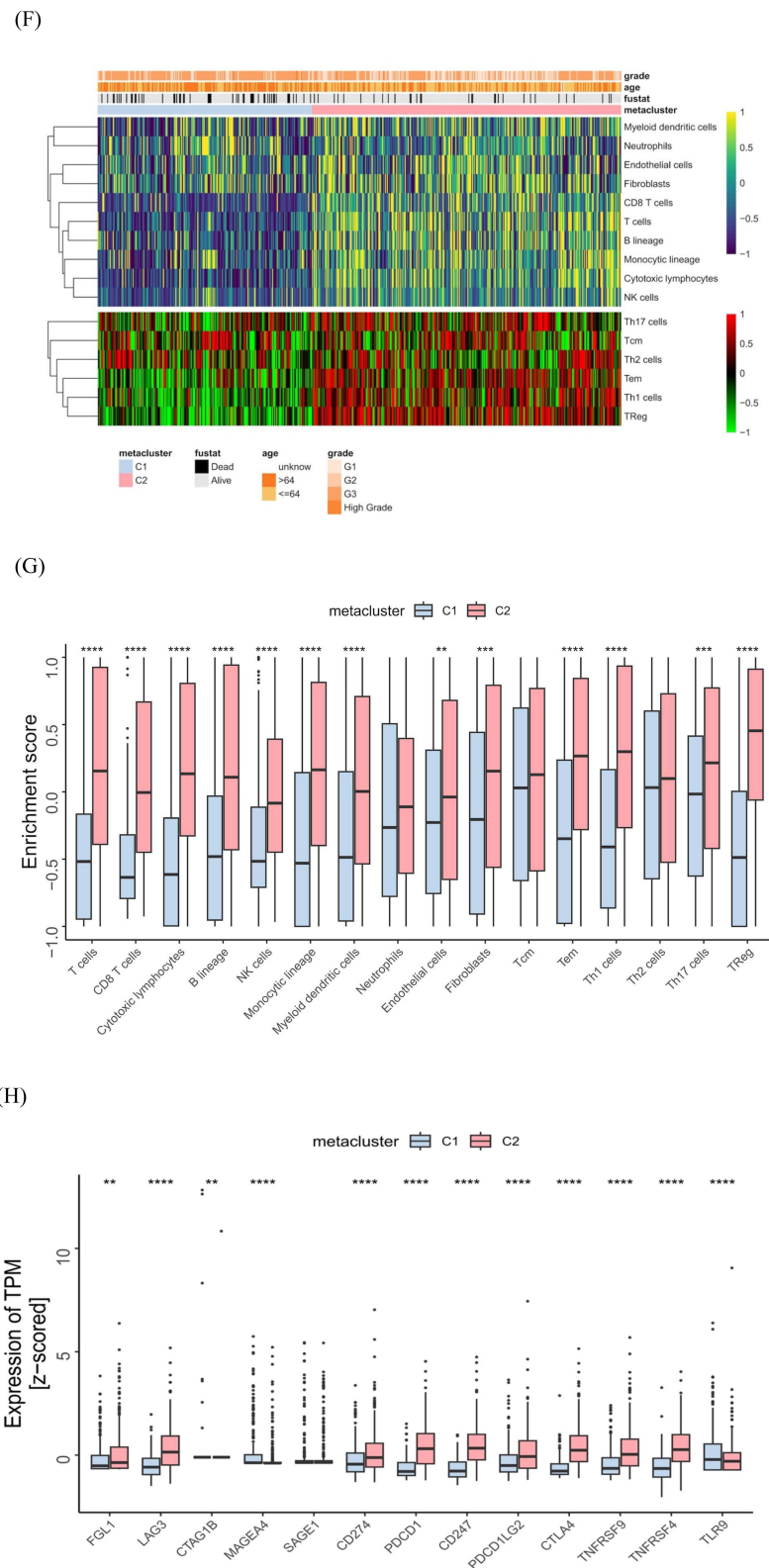
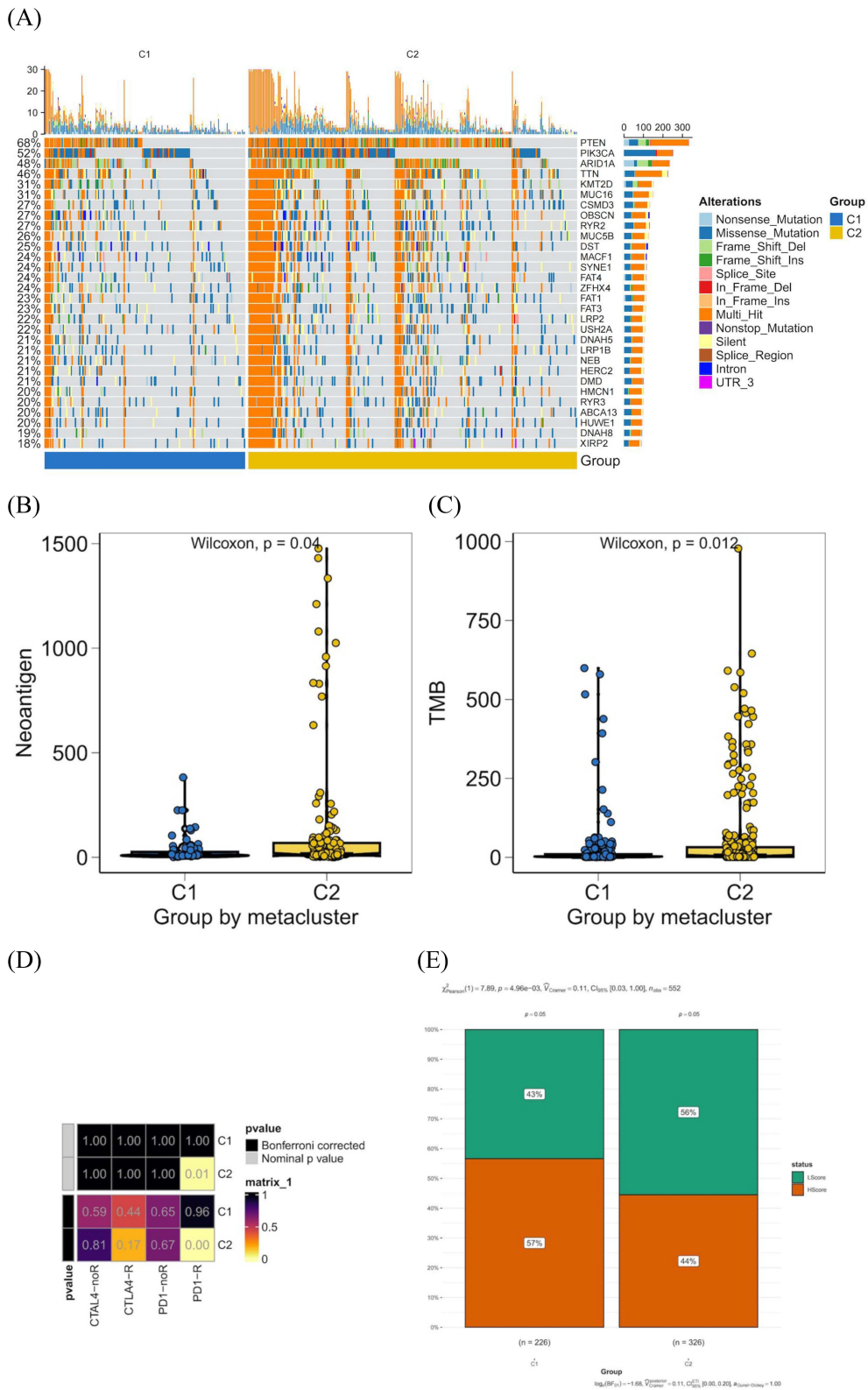


Figure 2 Continue.



**Figure 2** Characterization of immune subtypes. **(A)** Immune cells heatmap for metacluster in TCGA. **(B)** Boxplot for immune cells in metacluster of TCGA. **(C)** Boxplot for oncogenetic pathways in metacluster of TCGA. **(D)** Boxplot for immune score in metacluster of TCGA. **(E)** Boxplot for stromal score in metacluster of TCGA. **(F)** Comprehensive heatmap for MCPcounter and ssGSEA immune score. **(G)** Boxplot for immune signatures in metacluster of TCGA. **(H)** Boxplot for immune checkpoint targets in metacluster of TCGA. For boxplots, the line within the boxes, represents the median value, and the bottom and top of the boxes are the 25th and 75th percentiles (interquartile range), and the vertical line represents 1.5 times the interquartile range. The statistical difference was compared through the Kruskal–Wallis test, and the P values are labeled above each boxplot with asterisks (\*P < 0.05, \*\*P < 0.01, \*\*\*P < 0.001, \*\*\*\*P < 0.0001).





**Figure 3** Mutation, TMB and Immunotherapy. **(A)** Mutation profiles in C1 and C2. **(B)** Tumor neoantigen in C1 and C2. **(C)** TMB in C1 and C2. **(D)** C2 may be more sensitive to the PD-I inhibitor (nominal P = 0.01, Bonferroni corrected P < 0.01) by SubMap analysis. **(E)** The analysis of tumor immune rejection, Exclusion.

This model passed the calibration test, with  $p=0.634 > 0.05$  and Receiver operating characteristic area of 0.941, indicating that the key genes have good predictive ability for the immune subtype model. Furthermore, we conducted a univariate Cox regression analysis using Lasso regression to further construct a prognostic related model, incorporating the clinical

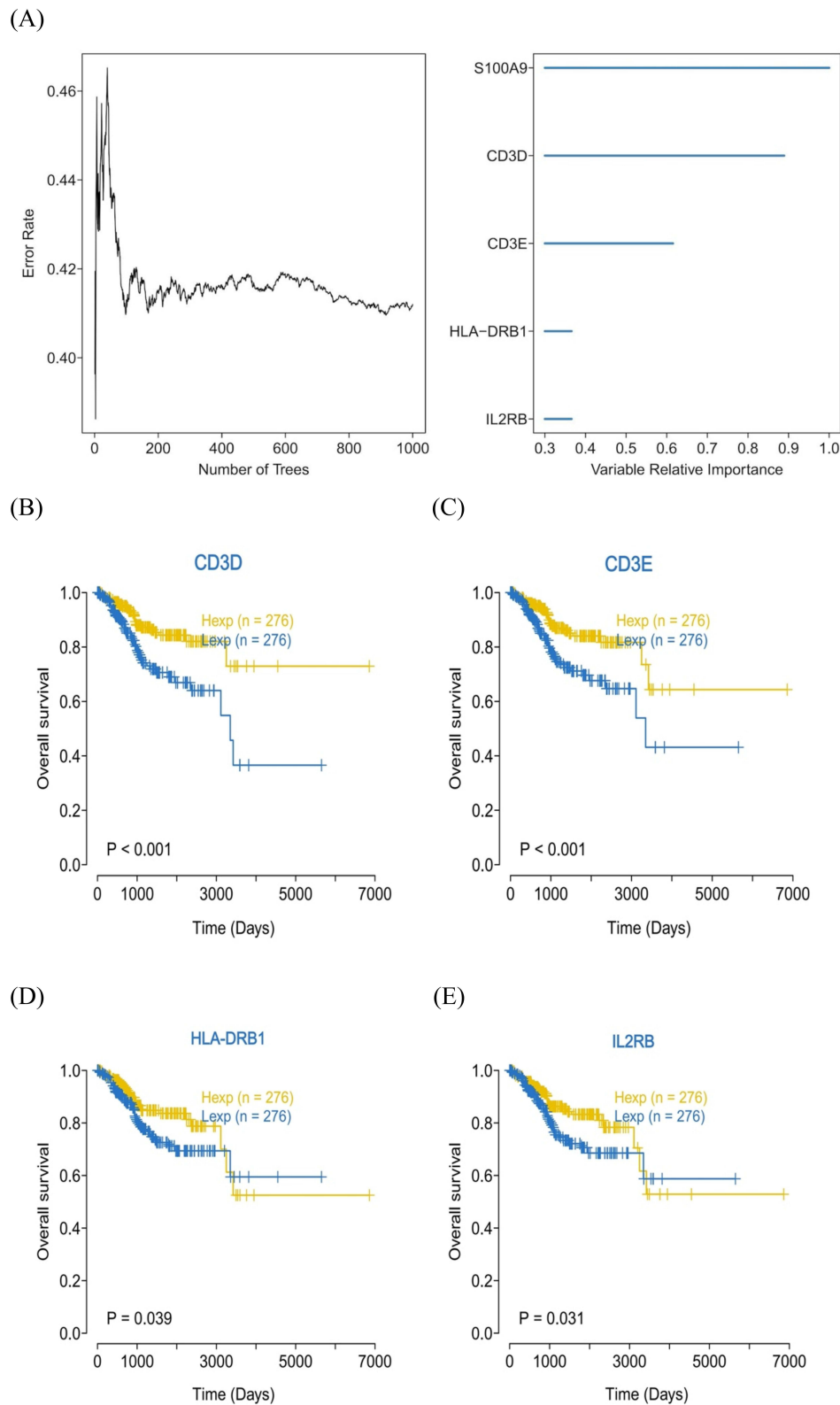
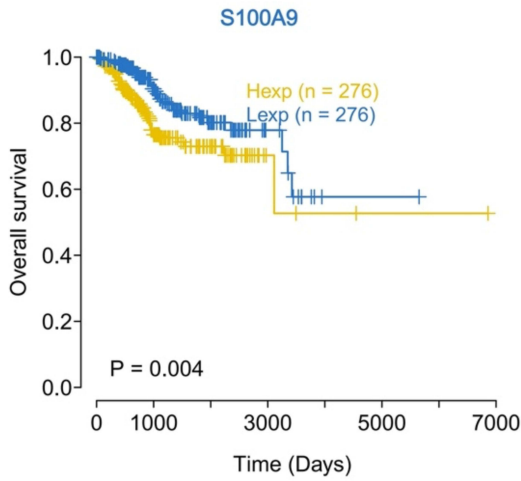
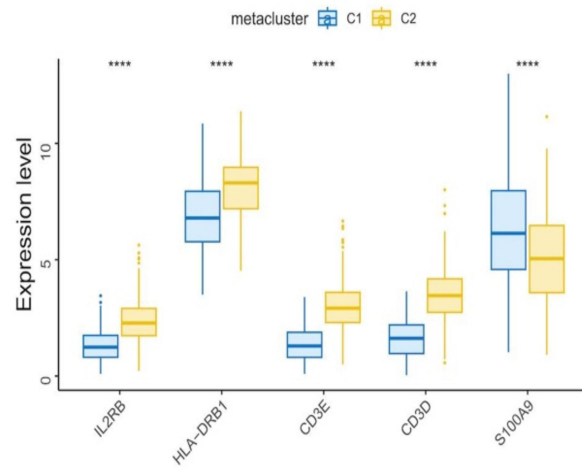


Figure 4 Continue.

(F)



(G)



(H)

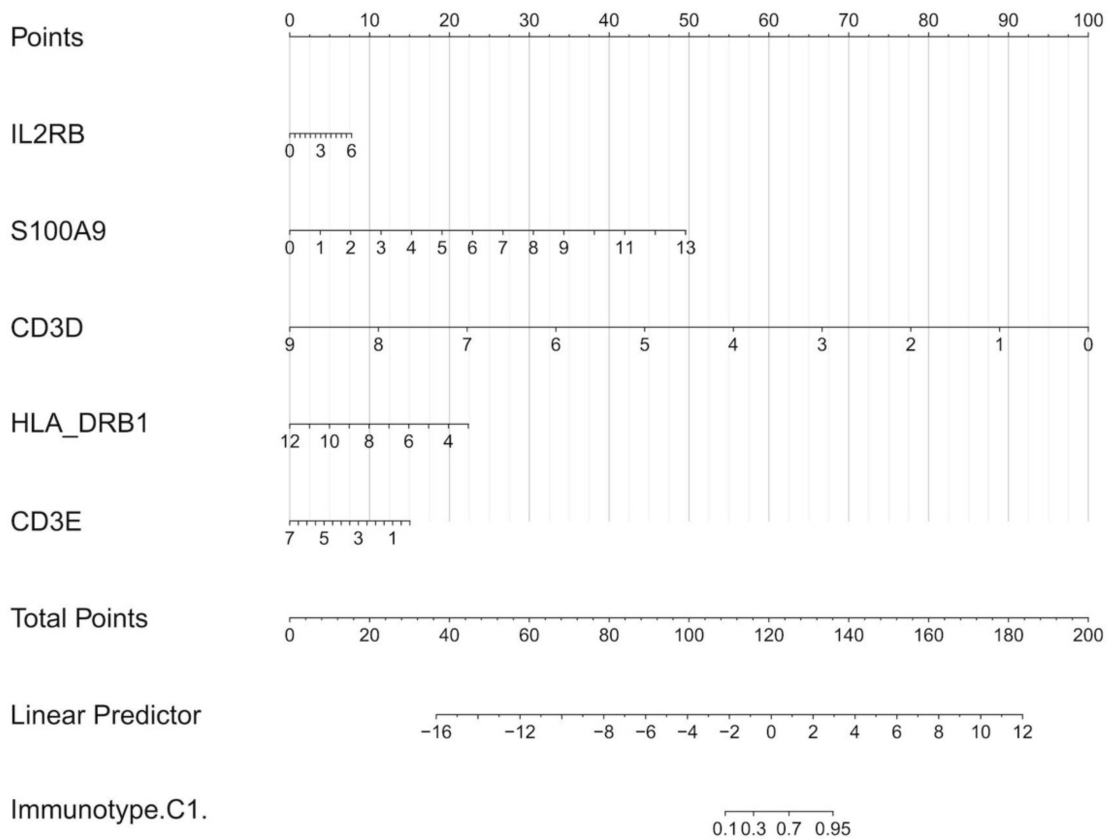
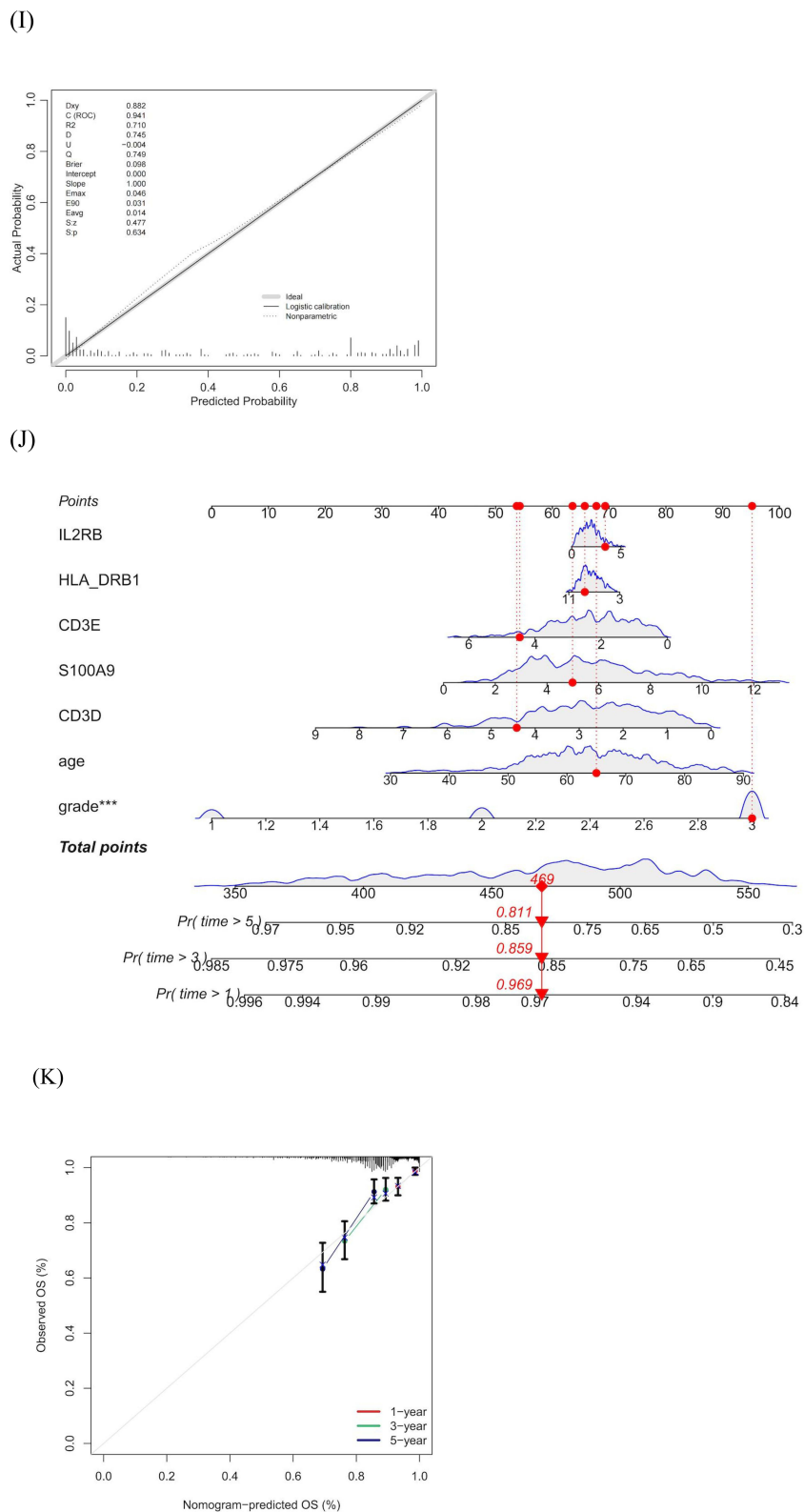


Figure 4 Continue.



**Figure 4** Key genes of immune subtype and prediction models for immune subtype and clinical prognosis. (A) Genes with relative importance >0.3 were identified as the final markers. (B) KM results of CD3D. (C) KM results CD3E. (D) KM results of HLA-DRB1. (E) KM results of IL2RB. (F) KM results of S100A9. (G) The expression levels of key genes in different subtypes. (H) The nomogram of the prognostic model for immune subtypes. (I) A calibration curve for verifying immune subtype model. (J) The nomogram of the clinical prognosis model. (K) Validation of the model for clinical prognosis.

characteristics, age and grade of patients. We combined key genes to construct a model for the prognosis of immune subtypes, and plotted a nomogram (Figure 4J). Using Bootstrap resampling method for internal validation based on the training set and plotting the calibration plot (Figure 4K). The C-index value of this model is 0.705, and the 1-year, 3-year, and 5-year survival curves are close to the dashed line, indicating good consistency of the model. This prognostic model has good predictive ability.

**qRT-PCR analysis:** In order to verify the expression of the key genes in EC tissues, we experimentally confirmed this by qRT-PCR using EC tumors and their adjacent normal tissues extracted from five patients. The qRT-PCR results and the clinical features of the five EC patients are shown in Figure 5. Three of the five patients were molecularly typed as NSMP and two as MMRd. S100A9, CD3D and HLA-DRB1 were all highly expressed in EC tissues compared with normal healthy control ( $p < 0.05$ , Student's  $t$ -test,  $n = 5$ ). The expression of IL2RB and CD3E did not reach the significance (Figure 5A). The observed trends in these results are largely consistent with those observed in the TCGA database (Figure 5B). Our experimental results demonstrated that the expression of the HLA-DRB1 was significantly higher in tumors than in normal tissues ( $p < 0.05$ ). In the TCGA database, the expression of the HLA-DRB1 tends to be higher in tumors than in normal tissues, although this does not reach statistical significance. These results indicate that our analysis is reliable.

**Relationship between immune subtypes and molecular subtypes:** A total of 538 EC patients with microsatellite stable status, gene mutations, copy number variations, clinical features and clinical outcomes were included in the TCGA-EC cohort (Table 1). The median age of C1 and C2 was 67 and 62 years, respectively, with a statistically significant difference ( $p < 0.0001$ ). In C1, the incidence rates of grade I and II were significantly lower than C2, and the incidence rate of grade III and IV was significantly higher than C2, both with statistical significance. ( $p < 0.05$ ) According to immune classification, there were 216 cases of C1 (40.15%) and 322 cases of C2 (59.85%). According to molecular classification, the highest number of patients among the 538 cases was the NSMP type with 178 cases (33.09%), followed by the TP53abn type with 145 cases (24.95%), the MSI-H type with 133 cases (24.72%) and the POLE type with 82 cases (15.24%). The TP53abn type had the highest number of C1 subtypes with a total of 91 cases (42.13%), followed by 63 cases (29.17%) of the NSMP type, 47 cases (21.76%) of the MSI-H type, and 15 cases (6.94%) of the POLE type. The NSMP type had the highest number of C2 subtypes with a total of 115 cases (35.71%), followed by the MSI-H type with 86 cases (26.7%), the POLE type with 67 cases (20.81%) and the TP53abn type with 54 cases (16.77%). The incidence of TP53abn type in C1 subtype is significantly higher than that in C2 subtype, while the incidence of POLE type is significantly lower than that in C2 subtype, and the difference is statistically significant ( $p < 0.0001$ ). The incidence of

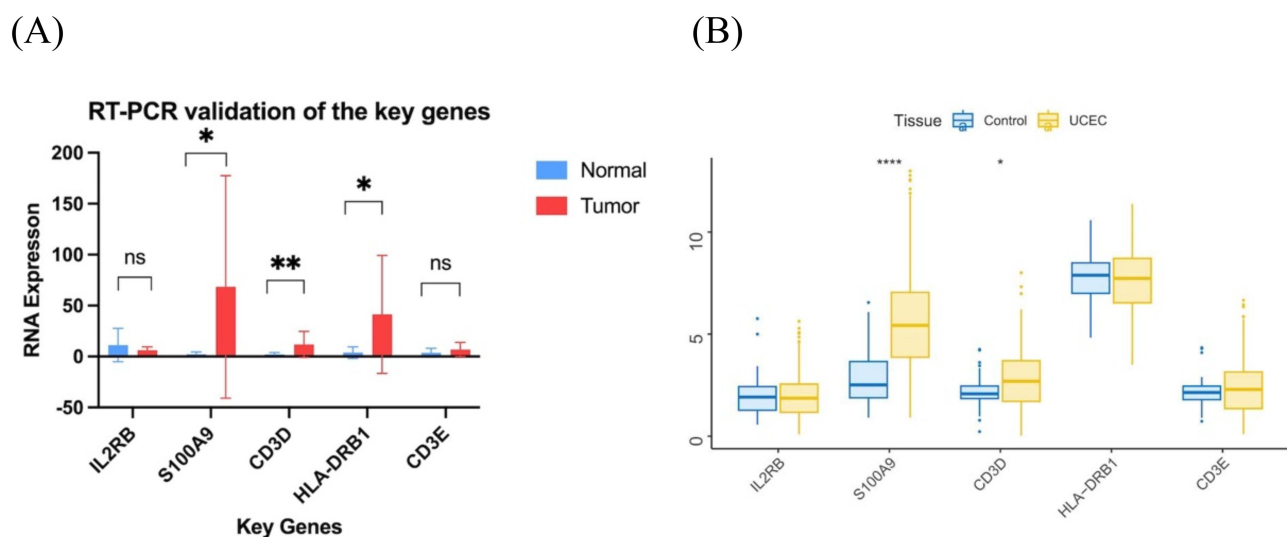


**Figure 5** qRT-PCR validation of the key genes. (A) RNA expression of key genes in qRT-PCR. (B) RNA expression of key genes from TCGA database. (\* $P < 0.05$ , \*\* $P < 0.01$ , \*\*\* $P < 0.0001$ ).



**Table I** Clinical Characteristics and Key Gene Expression Levels of Patients in the TCGA-EC Cohort

label	Variable	Immunotype Type		Total	Test
		C1 (N=216)	C2 (N= 322)		
Age (Year)	Min / Max	33.0 / 90.0	31.0 / 90.0	31.0 / 90.0	p <0.0001
	Med [IQR]	67.5 [60.0;74.0]	62.0 [55.0;69.0]	64.0 [57.0;71.0]	
	Mean**	67.2	61.7	63.9	
Grade	Grade I **	19 (8.78%)	80 (24.84%)	99 (18.40%)	p <0.0001
	Grade II *	34 (15.74%)	87 (20.19%)	121 (22.49%)	p <0.05
	Grade III and IV **	163 (75.46%)	155 (48.14%)	318 (59.10%)	p <0.0001
Molecular type	MSI-H	47 (21.76%)	86 (26.71%)	133 (24.72%)	p >0.05
	NSMP	63 (29.17%)	115 (35.71%)	178 (33.09%)	p >0.05
	POLE**	15 (6.94%)	67 (20.81%)	82 (15.24%)	p <0.0001
	TP53**	91 (42.13%)	54 (16.77%)	145 (26.95%)	p <0.0001
CD3D	Min / Max	0.04 / 3.6	0.6 / 8.0	0.04 / 8.0	p <0.0001
	Med [IQR]	1.6 [1.0;2.2]	3.4 [2.7;4.2]	2.7 [1.7;3.7]	
	Mean**	1.6	3.5	2.8	
CD3E	Min / Max	0.1 / 3.4	0.5 / 6.4	0.1 / 6.4	p <0.0001
	Med [IQR]	1.3 [0.8;1.9]	2.9 [2.3;3.6]	2.3 [1.4;3.2]	
	Mean**	1.4	3.0	2.3	
IL2RB	Min / Max	0.1 / 3.5	0.2 / 5.3	0.1 / 5.3	p <0.0001
	Med [IQR]	1.2 [0.8;1.7]	2.3 [1.7;2.9]	1.9 [1.2;2.5]	
	Mean**	1.3	2.3	1.9	
HLA_DRB1	Min / Max	3.5 / 10.9	4.5 / 11.2	3.5 / 11.2	p <0.0001
	Med [IQR]	6.8 [5.8;8.0]	8.3 [7.2;9.0]	7.8 [6.5;8.7]	
	Mean**	6.8	8.1	7.6	
S100A9	Min / Max	1.0 / 13.0	0.9 / 11.1	0.9 / 13.0	p <0.0001
	Med [IQR]	6.1 [4.6;8.0]	5.0 [3.6;6.4]	5.4 [3.8;7.0]	
	Mean**	6.5	5.1	5.7	

Notes: \* p <0.05; \*\*p<0.0001.

NSMP and MSI-H subtypes in C1 subtype showed a tendency to be lower than that in C2 subtype, but did not reach statistical significance ( $p > 0.05$ ). The expression levels of four key genes, CD3D, CD3E, IL2RB and HLA-DRB1, in C1 typing were significantly lower than those in C2, while the expression levels of S100A9 were significantly higher than those in C2, consistent with previous statistical results and with statistical significance ( $p < 0.0001$ ).

## Discussion

EC is an ideal candidate for immunotherapy. On the one hand, EC cells express Programmed Death Protein Ligand 1 (PD-L1) and Programmed Death Protein Ligand 2, which bind to PD-1 on tumor-infiltrating T-lymphocytes ( $CD4^+$ / $CD8^+$ ). This downregulates cellular immune responses through immune checkpoint mechanisms, allowing the tumor cells to ‘immuno-escape’.<sup>25,26</sup> Vanderstraeten et al proposed that between 67% and 100% of primary, recurrent and metastatic EC expressed PD-L1.<sup>27</sup> Conversely, in POLE-ultramutated and MMRd subtypes with high TMB, there is a correlation with high immunogenicity, which is evidenced by the presence of more tumor-associated specific neoantigens. This leads to an increase in  $CD3^+$  and  $CD8^+$  tumor-infiltrating lymphocytes, with the potential for compensatory up-regulation of immune checks and cytotoxic responses. Nevertheless, the relatively low rate of immune response has prompted us to consider whether there are new approaches to typing that could assist in the screening of immune populations for therapeutic advantages.<sup>28,29</sup>

Our study identified two distinct immune subtypes, C1 and C2. To validate the accuracy of subtypes, three external validation sets were employed. The level of B cells, T cells, T helper cells, Tem, and other related cells were significantly higher in the C2 subgroup than in the C1 subgroups. It has been demonstrated the presence of a large number of immune

cells and cytokines in EC tissues can stimulate endogenous anti-tumor immune responses.<sup>30</sup> Tumor-infiltrating immune cells can exert anti-tumor killing effects through specific immune responses mediated by cellular immunity, which may result in benefits for patients undergoing immunotherapy.<sup>31</sup> C2 was found to exhibit higher expression in immune checkpoints. Inhibition of immune checkpoint signaling pathways represents a promising avenue for accelerating the anti-tumor immune response, suggesting that C2 may be a particularly responsive target for immunotherapy.<sup>8</sup> Furthermore, our results indicated that the C2 subtype was more sensitive to common chemotherapeutic agents and immunotherapy. Analysis of tumor immune rejection revealed that C2 had a significantly lower immune exclusion response than C1, which further suggests greater sensitivity to immunotherapy, consistent with our results of immune cell infiltration and immune checkpoint expression.

Additionally, the mutation ratio of several genes including PTEN, PIK3CA, ARID1A, TTN, and Lysine-specific histone methyltransferase 2D was found to be significantly higher in C2 than in C1. Tumor neoantigens and tumor mutation load were found to be significantly higher in C2 than in C1. It is hypothesized that C2 has a highly immunogenic profile and may exhibit a great number of tumor-associated specific neoantigens, leading to an increase in infiltrating lymphocytes. This, in turn, has the potential for compensatory upregulation of the immune checkpoint and cytotoxic response.

We further used the RSF algorithm was employed to identify the core genes affecting immune subtypes and its prognosis. Finally, five key genes were identified affecting immune subtypes by RSF, which were S100A9, CD3D, CD3E, HLA-DRB1 and IL2RB in order of importance.

The S100s are a group of calcium-binding proteins comprising more than 20 members.<sup>32</sup> The dysregulated expression of S100 family members has been associated with the regulation of various cellular functions, including proliferation, apoptosis, migration, and differentiation of cancer cells.<sup>33,34</sup> Zhang et al reported that the expression levels of S100A2, S100A7, S100A7A, S100A8, S100A9, and S100A14 were significantly higher in EC and were also associated with the OS of patients.<sup>35</sup> Furthermore, S100s has been reported to interact with the IL-17 signalling pathway. The production of cytokines and chemokines is regarded as being promoted by the IL-17 signalling cascade. Following the formation of a bond with its receptor, IL-17 triggers mitogen-activated protein kinases, resulting in the release of inflammatory mediators such as IL-6, IL-1, and BNF- $\kappa$ B 34. Chen et al have previously demonstrated that S100A9 has the potential to be utilised as a tumor diagnostic or prognostic biomarker.<sup>36</sup> In our study, S100A9 gene expression was found to be lower in the C2 group than in C1 ( $p < 0.05$ ). This is consistent with previous studies which have demonstrated that OS is significantly higher in C2 than in C1.

IL2RB, which is also known as CD122, has been implicated in both T-cell expansion and exhaustion.<sup>37</sup> Phase II/III clinical trials in patients with advanced solid tumors are currently investigating IL2RB as a promising therapeutic target in combination with immune-checkpoint blockade.<sup>38</sup> Alderdice et al identified IL2RB as being widely associated with immune-checkpoints in colorectal cancer and its expression should be investigated for clinical utility as a potential predictive biomarker for colorectal cancer patients receiving immune-checkpoint blockade.<sup>39</sup> To date, there is no literature reporting the relationship between IL2RB and EC. Based on the role of this gene in colorectal cancer, it can be postulated that perhaps this gene may also be a target for EC treatment. However, further studies are required to confirm this hypothesis. HLA-DRB1 which is responsible for antigen presentation to CD4+ T cells, has been reported to be associated with many types of autoimmune diseases.<sup>40-42</sup> To date, no literature has been published on the relationship between HLA-DRB1 and EC. As HLA-DRB1 is immune-related, our study showed that subtype C2 has more pronounced immune characteristics and is more sensitive to immunotherapy, suggesting that our results are consistent with previous studies. It may be hypothesized that HLA-DRB1 is a target for future immunotherapy. The CD3 antigen is a crucial marker on the surface of T cells, comprising four protein chains: CD3  $\delta$ ,  $\epsilon$ ,  $\gamma$  and  $\zeta$ . The heterodimeric CD3  $\epsilon$  -  $\gamma$  and CD3  $\epsilon$  -  $\delta$  form TCR-CD3 complexes with the alpha/beta chains of TCR. The histocompatibility protein complex (MHC) presented by antigen-presenting cells (APCs) can interact with the TCR-CD3 complex to induce T cell activation. The TCR-CD3 complex is a pivotal molecule that initiates T cell activation and differentiation, and may result in disparate outcomes contingent upon the quantity and quality of stimulation.<sup>43</sup> This may account for the low response rate observed in MMRd patients with particularly high PD-L1 expression to ICIs. If T cells are impeded during activation, subsequent immune checkpoints are unable to function. Consequently, CD3D and CD3E may represent another potential

target for immunotherapy. A number of studies have demonstrated that CD3D and CD3E are closely related to the occurrence, development, prognosis, immune microenvironment and treatment response of tumors.<sup>44</sup> Kang et al have shown that CD3D expression is associated with a worse prognosis in bladder cancer.<sup>45</sup> The association between high CD3E expression and a better prognosis in ovarian cancer patients was reported by Huo.<sup>46</sup> According to Saiz-Ladera, CD3D and CD3E were linked to improved outcomes in patients with head and neck squamous cell carcinoma patients and an increase in infiltrating immune effector cells.<sup>47</sup> Zhang et al also reported that low expression of the hub genes CD3D and CD3E was associated with poor prognosis in ovarian cancer.<sup>48</sup> These genes may play a role not only as biomarkers for predicting prognosis, but also as potential targets for immunotherapy. Based on our results, we also believe that high expression of CD3D and CD3E is a marker for good prognosis in EC and a potential target for immunotherapy.

The innovation of this study lies in its exploration of the relationship between immune subtypes and four molecular subtypes. In 2013, TCGA pioneered the molecular typing of EC, with 373 cases of POLE-ultramutated, MSI-H or MMRd, CNL or NSMP and CNH or TP53 subtypes, accounting for 7%, 28%, 39%, and 26%, respectively.<sup>6</sup> The prognosis of POLE-ultramutated patients is favorable, even in the absence of adjuvant therapy following surgical intervention.<sup>49</sup> The prognosis of MSI-H/MMRd patients is moderate and NCCN guidelines in the US recommended patients with MSI-H/MMRd consider pembrolizumab or dostarlimab as a first-line treatment option.<sup>9</sup> The NSMP type has the highest number of cases among the four subtypes and its prognosis is worse than MSI-H/MMRd and POLE-ultramutated types.<sup>50</sup> Furthermore TP53 patients have the worst prognosis, the treatment of the two subtypes is currently uncertain.<sup>50</sup> Consequently, molecular typing cannot, to some extent, screen the most suitable population for immunotherapy. Our study revealed that the incidence of POLE in the C2 subtype, which is more sensitive to immunotherapy, is significantly higher than that of C1, while the incidence of TP53 is significantly lower than that of C1. Nevertheless, no significant difference was observed in the incidence of MSI-H and NSMP between the two groups. This implies that, even in clinical practice, there is a possibility that patients with MSI-H subtypes may not respond to immunotherapy. This result is consistent with the previously published immunotherapeutic effects on MMRd. In our study, 133 cases of MSI-H were identified, with C1 accounting for 47 cases (35.34%) and C2 accounting for 86 cases (67.66%). These findings indicate that molecular typing alone has limitations in predicting immunotherapy. Among the 538 patients in the study, the NSMP type exhibited the greatest diversity in molecular subtypes, with 178 cases (33.09%), of which C1 accounted for 63 cases (35.39%) and C2 accounted for 86 cases (64.61%). This indicates that if the immune subtypes of these patients can be identified, then the appropriate immunotherapy may be administered.

The results of the preceding analysis led to the construction of a model for predicting immune subtypes. This model was constructed using five key logistic regression methods, which were further refined by incorporating patient age and grading. In addition, key genes were combined to construct a model for predicting the prognosis of immune subtypes. Both models demonstrate satisfactory predictive capacity. In clinical practice, the immune subtypes of EC patients may be identified by detecting five key genes, a strategy that has consistently informed clinical decision-making.

This study had many innovative aspects. Firstly, we explored the potential immune subtypes of EC by immune-related genes, and validated them by multiple external datasets and perspectives. Secondly, we investigated the immune classification and its key genes through multi-omics methods and multi-angle analysis, which provided reliable ideas for the treatment and prognosis of EC patients. Thirdly, we utilise key genes to construct a model for predicting immune subtypes, and combine clinical features to construct a model for predicting immune subtypes prognosis. Finally, the most significant aspect of this study is the investigation of the relationship between immune subtypes and molecular subtypes. This not only highlights the limitations of molecular subtypes in the clinical treatment of EC, but also demonstrates the significance of immune subtypes in clinical practice. We also have limitations. Our data were obtained from a public database and were based on a retrospective analysis. Therefore, further prospective studies are needed in the future to validate the immune subtypes of EC.

## Conclusion

In summary, we have identified two immune subtypes with distinct immune characteristics. S100A9, CD3D, CD3E, HLA-DRB1 and IL2RB are the key genes of the immune subtypes. Low expression of S100A9 and high expression of

IL2RB, HLA-DRB1, CD3E, and CD3D indicate a favorable prognosis and sensitivity to immunotherapy. This information may have both prognostic and predictive value, as well as guiding future immunotherapy.

## Ethical Statement

This study was performed in line with the principles of the Declaration of Helsinki. Approval was granted by the Ethics Committee of Beijing Obstetrics and Gynecology Hospital (2024-KY-037-01). Informed consent was obtained from all participants.

## Funding

This work was supported by Capital's Funds for Health Improvement and Research (Grant numbers No.2024-1-2112).

## Disclosure

The authors report no conflicts of interest in this work.

## References

- Sung H, Ferlay J, Siegel RL, et al. Global cancer statistics 2020: GLOBOCAN estimates of incidence and mortality worldwide for 36 cancers in 185 countries. *CA Cancer J Clin.* 2021;71:209–249. doi:10.3322/caac.21660
- Siegel RL, Miller KD, Jemal A. Cancer statistics, 2018. *CA Cancer J Clin.* 2018;68:7–30. doi:10.3322/caac.21442
- Zheng R, Zhang S, Zeng H, et al. Cancer incidence and mortality in China, 2016. *J Nat Cancer Center.* 2022;2:1–9. doi:10.1016/j.jncc.2022.02.002
- Colombo N, Creutzberg C, Amant F, et al.; Group E-E-EECCW. ESMO-ESGO-ESTRO consensus conference on endometrial cancer: diagnosis, treatment and follow-up. *Int J Gynecol Cancer.* 2016;26:2–30. doi:10.1097/IGC.0000000000000609
- Wilkinson-Ryan I, Binder PS, Pourabolghasem S, et al. Concomitant chemotherapy and radiation for the treatment of advanced-stage endometrial cancer. *Gynecol Oncol.* 2014;134:24–28. doi:10.1016/j.ygyno.2014.05.002
- Kandoth C, Schultz N, Cherniack AD, et al.; Cancer Genome Atlas Research N. Integrated genomic characterization of endometrial carcinoma. *Nature.* 2013;497:67–73.
- Jiang F, Jiang S, Cao D, Mao M, Xiang Y. Immunologic signatures across molecular subtypes and potential biomarkers for sub-stratification in endometrial cancer. *Int J Mol Sci.* 2023;25:24. doi:10.3390/ijms25010024
- Carlson JW, Nastic D. High-grade endometrial carcinomas: classification with molecular insights. *Surg Pathol Clin.* 2019;12:343–362. doi:10.1016/j.path.2019.02.003
- National Comprehensive Cancer Network. NCCN clinical practice guidelines in oncology (NCCN Guidelines): uterine neoplasms (Version 2.2023) [EB/OL]. Available from: [https://www.nccn.org/professionals/physician\\_gls/pdf/uterine.pdf](https://www.nccn.org/professionals/physician_gls/pdf/uterine.pdf). Accessed October 26, 2024.
- Liu J, Chen X, Jiang Y, Cheng W. Development of an immune gene prognostic classifier for survival prediction and respond to immunotherapy/chemotherapy in endometrial cancer. *Int Immunopharmacol.* 2020;86:106735. doi:10.1016/j.intimp.2020.106735
- Li BL, Wan XP. Prognostic significance of immune landscape in tumour microenvironment of endometrial cancer. *J Cell Mol Med.* 2020;24:7767–7777. doi:10.1111/jcmm.15408
- Bagaev A, Kotlov N, Nomie K, et al. Conserved pan-cancer microenvironment subtypes predict response to immunotherapy. *Cancer Cell.* 2021;39:845–857. doi:10.1016/j.ccell.2021.04.014
- Thorsson V, Gibbs DL, Brown SD, et al. The immune landscape of cancer. *Immunity.* 2018;48:812–830. doi:10.1016/j.immuni.2018.03.023
- Cai Y, Chang Y, Liu Y. Multi-omics profiling reveals distinct microenvironment characterization of endometrial cancer. *Biomed Pharmacother.* 2019;118:109244. doi:10.1016/j.biopha.2019.109244
- Wang G, Wang D, Sun M, Liu X, Yang Q. Identification of prognostic and immune-related gene signatures in the tumor microenvironment of endometrial cancer. *Int Immunopharmacol.* 2020;88:106931. doi:10.1016/j.intimp.2020.106931
- Mariathasan S, Turley SJ, Nickles D, et al. TGFbeta attenuates tumour response to PD-L1 blockade by contributing to exclusion of T cells. *Nature.* 2018;554:544–548. doi:10.1038/nature25501
- Possemato R, Marks KM, Shaul YD, et al. Functional genomics reveal that the serine synthesis pathway is essential in breast cancer. *Nature.* 2011;476:346–350. doi:10.1038/nature10350
- Barbie DA, Tamayo P, Boehm JS, et al. Systematic RNA interference reveals that oncogenic KRAS-driven cancers require TBK1. *Nature.* 2009;462:108–112. doi:10.1038/nature08460
- Yoshihara K, Shahmoradgoli M, Martinez E, et al. Inferring tumour purity and stromal and immune cell admixture from expression data. *Nat Commun.* 2013;4:2612. doi:10.1038/ncomms3612
- Becht E, Giraldo NA, Lacroix L, et al. Estimating the population abundance of tissue-infiltrating immune and stromal cell populations using gene expression. *Genome Biol.* 2016;17:218. doi:10.1186/s13059-016-1070-5
- Ritchie ME, Phipson B, Wu D, et al. limma powers differential expression analyses for RNA-sequencing and microarray studies. *Nucleic Acids Res.* 2015;43:e47. doi:10.1093/nar/gkv007
- Yang W, Soares J, Greninger P, et al. Genomics of drug sensitivity in cancer (GDSC): a resource for therapeutic biomarker discovery in cancer cells. *Nucleic Acids Res.* 2013;41:D955–61. doi:10.1093/nar/gks1111
- Jiang P, Gu S, Pan D, et al. Signatures of T cell dysfunction and exclusion predict cancer immunotherapy response. *Nat Med.* 2018;24:1550–1558. doi:10.1038/s41591-018-0136-1
- Cai HQ, Zhang MJ, Cheng ZJ, et al. FKBP10 promotes proliferation of glioma cells via activating AKT-CREB-PCNA axis. *J Biomed Sci.* 2021;28:13. doi:10.1186/s12929-020-00705-3

25. Mo Z, Liu J, Zhang Q, et al. Expression of PD-1, PD-L1 and PD-L2 is associated with differentiation status and histological type of endometrial cancer. *Oncol Lett.* 2016;12:944–950. doi:10.3892/ol.2016.4744
26. Kucukgoz Gulec U, Kilic Bagir E, Paydas S, Guzel AB, Gumurdulu D, Vardar MA. Programmed death-1 (PD-1) and programmed death-ligand 1 (PD-L1) expressions in type 2 endometrial cancer. *Arch Gynecol Obstet.* 2019;300:377–382. doi:10.1007/s00404-019-05180-2
27. Vanderstraeten A, Luyten C, Verbist G, Tuyaerts S, Amant F. Mapping the immunosuppressive environment in uterine tumors: implications for immunotherapy. *Cancer Immunol Immunother.* 2014;63:545–557. doi:10.1007/s00262-014-1537-8
28. Konstantinopoulos PA, Luo W, Liu JF, et al. Phase II study of avelumab in patients with mismatch repair deficient and mismatch repair proficient recurrent/persistent endometrial cancer. *J Clin Oncol.* 2019;37(30):2786–2794. doi:10.1200/JCO.2019.010121
29. Antill YC, Kok PS, Robledo K, et al. Activity of durvalumab in advanced endometrial cancer (AEC) according to mismatch repair (MMR) status: the phase II PHAEDRA trial (ANZGOG1601). *JCO.* 2019;37(15\_suppl):5501. doi:10.1200/JCO.2019.37.15\_suppl.5501
30. Dyck L, Prendeville H, Raverdeau M, et al. Suppressive effects of the obese tumor microenvironment on CD8 T cell infiltration and effector function. *J Exp Med.* 2022;219:1.
31. van der Woude H, Hally KE, Currie MJ, Gasser O, Henry CE. Importance of the endometrial immune environment in endometrial cancer and associated therapies. *Front Oncol.* 2022;12:975201. doi:10.3389/fonc.2022.975201
32. Nakayama S, Kretsinger RH. Evolution of the EF-hand family of proteins. *Annu Rev Biophys Biomol Struct.* 1994;23:473–507. doi:10.1146/annurev.bb.23.060194.002353
33. Leclerc E, Vetter SW. The role of S100 proteins and their receptor RAGE in pancreatic cancer. *Biochim Biophys Acta.* 2015;1852:2706–2711. doi:10.1016/j.bbdis.2015.09.022
34. Allgower C, Kretz AL, von Karstedt S, Wittau M, Henne-Bruns D, Lemke J. Friend or foe: S100 proteins in cancer. *Cancers.* 2020;13:12. doi:10.3390/cancers13010012
35. Zhang Q, Xia T, Qi C, Du J, Ye C. High expression of S100A2 predicts poor prognosis in patients with endometrial carcinoma. *BMC Cancer.* 2022;22:77. doi:10.1186/s12885-022-09180-5
36. Chen Y, Ouyang Y, Li Z, Wang X, Ma J. S100A8 and S100A9 in Cancer. *Biochim Biophys Acta Rev Cancer.* 2023;1878:188891. doi:10.1016/j.bbcan.2023.188891
37. Charych D, Khalili S, Dixit V, et al. Modeling the receptor pharmacology, pharmacokinetics, and pharmacodynamics of NKTR-214, a kinetically-controlled interleukin-2 (IL2) receptor agonist for cancer immunotherapy. *PLoS One.* 2017;12:e0179431. doi:10.1371/journal.pone.0179431
38. Garber K. Cytokine resurrection: engineered IL-2 ramps up immuno-oncology responses. *Nat Biotechnol.* 2018;36:378–379. doi:10.1038/nbt0518-378
39. Alderdice M, Craig SG, Humphries MP, et al. Evolutionary genetic algorithm identifies IL2RB as a potential predictive biomarker for immune-checkpoint therapy in colorectal cancer. *NAR Genom Bioinform.* 2021;3:lqab016. doi:10.1093/nargab/lqab016
40. Liu S, Li Q, Zhang Y, et al. Association of human leukocyte antigen DRB1\*15 and DRB1\*15:01 polymorphisms with response to immunosuppressive therapy in patients with aplastic anemia: a meta-analysis. *PLoS One.* 2016;11:e0162382. doi:10.1371/journal.pone.0162382
41. Niu Z, Zhang P, Tong Y. Value of HLA-DR genotype in systemic lupus erythematosus and lupus nephritis: a meta-analysis. *Int J Rheum Dis.* 2015;18:17–28. doi:10.1111/1756-185X.12528
42. Ji C, Liu S, Zhu K, et al. HLA-DRB1 polymorphisms and alopecia areata disease risk: a systematic review and meta-analysis. *Medicine.* 2018;97:e11790. doi:10.1097/MD.00000000000011790
43. Zhang R, Zhang J, Zhou X, Zhao A, Yu C. The establishment and application of CD3E humanized mice in immunotherapy. *Exp Anim.* 2022;71:442–450. doi:10.1538/expanim.22-0012
44. Yuan L, Xu J, Shi Y, et al. CD3D is an independent prognostic factor and correlates with immune infiltration in gastric cancer. *Front Oncol.* 2022;12:913670. doi:10.3389/fonc.2022.913670
45. Kang Z, Li W, Yu YH, et al. Identification of immune-related genes associated with bladder cancer based on immunological characteristics and their correlation with the prognosis. *Front Genet.* 2021;12:763590. doi:10.3389/fgene.2021.763590
46. Huo X, Sun H, Liu S, et al. Identification of a prognostic signature for ovarian cancer based on the microenvironment genes. *Front Genet.* 2021;12:680413. doi:10.3389/fgene.2021.680413
47. Saiz-Ladera C, Baliu-Pique M, Cimas FJ, et al. Transcriptomic correlates of immunologic activation in head and neck and cervical cancer. *Front Oncol.* 2021;11:714550. doi:10.3389/fonc.2021.714550
48. Zhang M, Shi M, Yu Y, et al. The immune subtypes and landscape of advanced-stage ovarian cancer. *Vaccines.* 2022;11(1):10. doi:10.3390/vaccines11010010
49. Van Gool IC, Rayner E, Osse EM, et al. Adjuvant treatment for POLE proofreading domain-mutant cancers: sensitivity to radiotherapy, chemotherapy, and nucleoside analogues. *Clin Cancer Res.* 2018;24(13):3197–3203. doi:10.1158/1078-0432.CCR-18-0266
50. Bosse T, Nout RA, McAlpine JN, et al. Molecular classification of grade 3 endometrioid endometrial cancers identifies distinct prognostic subgroups. *Am J Surg Pathol.* 2018;42(5):561–568. doi:10.1097/PAS.0000000000001020

## Cancer Management and Research

Dovepress

### Publish your work in this journal

Cancer Management and Research is an international, peer-reviewed open access journal focusing on cancer research and the optimal use of preventative and integrated treatment interventions to achieve improved outcomes, enhanced survival and quality of life for the cancer patient. The manuscript management system is completely online and includes a very quick and fair peer-review system, which is all easy to use. Visit <http://www.dovepress.com/testimonials.php> to read real quotes from published authors.

Submit your manuscript here: <https://www.dovepress.com/cancer-management-and-research-journal>